

Paleoecology of the Camp Century Subglacial Sediment Core, Northwest Greenland

A thesis proposal prepared by

Halley M. Mastro

In partial fulfillment of the requirements for the degree of Master of Science in the Rubenstein
School of Environment and Natural Resources at the University of Vermont

The following are members of the thesis committee:

Paul R. Bierman, PhD, Advisor

Cathy Paris, PhD, Chair

Ana Morales-Williams, PhD

Abstract

Understanding responses of arctic vegetation and the Greenland Ice Sheet to climatic changes in the past holds global importance in evaluating ice sheet stability and potential contributions to sea level rise in the future. The history of the Greenland Ice Sheet beyond the last interglaciation has most often been interpreted through indirect marine records because terrestrial evidence is rare and inaccessible. The 1390 m Camp Century ice core, drilled in northwest Greenland from 1961-1966, retrieved 3.44 meters of frozen subglacial sediment with deposition spanning the Pleistocene. Organic remains, including plant and invertebrate macrofossils, are well-preserved in the sediment. My work will characterize past ice-free ecosystems and environments of northwest Greenland through macrofossil identification, stable isotope geochemistry of bulk organic material, and total carbon and nitrogen measurements of organic material and pore ice meltwater within the Camp Century subglacial sediment.

Initial identifications of plant and invertebrate specimens align with taxa represented in modern arctic tundra communities. General trends in carbon-nitrogen (C:N) ratios and stable isotope ratios of carbon indicate a shift in the dominant input of organic material from terrestrial C₃ plants to admixed aquatic and terrestrial material with decreasing core depth. Ongoing higher-level identifications of this material will provide more nuanced insight into the paleoenvironmental, and paleoclimate conditions preserved in this unique archive. The presence of abundant plant and invertebrate remains in the Camp Century subglacial sediment provides direct terrestrial evidence for sustained ice absence and the consequent development of a diverse ecological community in northwest Greenland during at least one Pleistocene interglacial period.

1. Introduction

Anthropogenic greenhouse gas emissions are altering global climate with disproportionately large impacts in the Arctic (Post et al., 2019). During the last decade, global mean surface temperature reached 1.1°C above pre-industrial levels (IPCC, 2022). Since 1979, the Arctic has been warming almost four times faster than the global average (Rantanen et al., 2022). In Greenland, rapid warming coupled with changing precipitation regimes has resulted in extensive landscape-level changes in both the cryosphere and biosphere (Schaeffer et al., 2013). Greenland Ice Sheet mass loss poses a potential contribution to global sea level rise of up to 7 meters, alters cryosphere-albedo feedback mechanisms, and could change global oceanic circulation patterns (Box et al., 2022; Briner et al., 2020; Hofer et al., 2020; Irvali et al., 2020).

Beyond the ice sheet, a spectral greening trend has been observed in the Arctic over the last 40 years, interpreted from satellite data as changes in vegetation type, distribution, and abundance (Myers-Smith et al., 2020; Myneni et al., 1997). This phenomenon, known as ‘Arctic greening’, influences vegetation-climate feedback mechanisms through lowering terrestrial albedo, increasing evapotranspiration, hindering permafrost thaw, and altering carbon dioxide

absorption and nutrient cycling (Crump et al., 2021; Elmendorf et al., 2012; Myers-Smith et al., 2020; Schaeffer et al., 2013). The interactions and implications of vegetative climate forcings are not fully understood due to heterogeneity in trends of vegetation change across arctic regions and limited in-situ observations to validate satellite-derived indices (Forkel et al., 2016; Lawrence & Swenson, 2011; Mekonnen et al., 2018; Pearson et al., 2013; Stone & Lunt, 2013; Sturm et al., 2001; Swann et al., 2010). Thus, the influence that ice-albedo and vegetation-climate feedback mechanisms in Greenland will have on the rate and severity of climate change remains uncertain.

Paleoclimate archives bridge this knowledge gap because they record how ice presence and vegetation moderated or amplified Arctic responses to past climatic changes. Pollen records from offshore marine sediments have been used to infer multiple periods of substantial ice sheet reduction and boreal forest development in southern Greenland over the last million years (de Vernal & Hillaire-Marcel, 2008; Steig & Wolfe, 2008). However, potential long-distance pollen grain transport by wind poses a challenge in reconstructing local vegetation history using these records exclusively (Birks, 1993).

Lacustrine and terrestrial sediment deposits bearing biotic remains beyond the current ice extent provide more direct reconstructions of former vegetation and environmental transitions through the most recent period of Arctic warming before present, the last interglacial (116,000-129,000 years ago) (Axford et al., 2011; Crump et al., 2021; Wagner & Bennike, 2012). Rare sediment deposits containing well-preserved floral and faunal remains (and in one case, DNA) around coastal Greenland record periods of ice sheet reduction with vegetation development from arctic to subarctic to boreal forest during the Early Pleistocene (~2-2.4 million years ago.) (Bennike et al., 2010, 2022; Bennike & Böcher, 1990; Funder et al., 1985, 2001; Kjær et al., 2022). The Pleistocene climate history of Greenland remains relatively uncertain, as preservation of such intact fossil-bearing terrestrial or lacustrine sedimentary sequences older than the most recent glaciation is uncommon due to subglacial erosion (Crump et al., 2021).

Ice core basal materials can provide direct paleoclimate records of smaller-than-present Greenland Ice Sheet configurations. Biomolecules, diatoms, and gas isotopes signifying biological activity from basal sections of the GRIP, Camp Century, and DYE-3 deep ice cores have yielded paleoenvironmental insights in areas of Greenland currently underneath kilometers of ice (Harwood, 1986; Souchez et al., 2006; Willerslev et al., 2007). Biotic proxies in ice core basal materials are difficult to obtain, and rarely contain well-preserved, robust indicators of

vegetation presence. The Camp Century subglacial sediment core is an exception because it contains abundant intact macrofossil remains and organic materials that have not yet been thoroughly studied (Christ et al., 2021).

My thesis research will directly characterize Pleistocene ecosystems of northwest Greenland using the biotic material within the Camp Century subglacial sediment archive, deposited at and before 416 ± 38 ka (Christ et al., 2023). This work will provide insight into local paleoenvironmental conditions during ice-free periods at Camp Century and contribute to scientific understanding of vegetation-climate interactions at high latitudes.

2. Background

2.1 Quaternary Greenland Climate History

Understanding climate conditions during past interglaciations, specifically those warmer than present, is consequential in determining modern responses of ice sheets to human-driven global climate change. Since ~ 2.6 Ma, the beginning of the Quaternary Period, cyclic alternations between glacial and interglacial periods characterized by Northern Hemisphere land-ice volume, global sea level, and boreal summer insolation are recorded in continuous terrestrial and marine climate records (Berger et al., 2016). The dominant periodicity of these cycles shifted from 41 ka to 100 ka between 1.2- 0.7 Ma, along with an intensification of the amplitude of oxygen isotopic signals of continental ice volume and temperature, known as the mid-Pleistocene transition (Elderfield et al., 2012).

Following this transition, interglaciations with lower-than-present global land-ice volume and higher-than-present global mean sea level are recorded in marine foraminifera and ice core oxygen isotope records, including Marine Isotope Stage (MIS) 11c, MIS 9e, MIS 7e and MIS 5e (Dutton et al., 2015; Elderfield et al., 2012). Although the four last interglaciations (MIS 11c: 394-424 ka, MIS 9e: 320-333 ka, MIS 7e: 232-243 ka, MIS 5e: 117-128 ka) reached temperatures warmer than today near southern Greenland, both the degree and duration of warmer than present conditions, and thus the Greenland Ice Sheet response, varied between them (Irvali et al., 2020).

Global climate feedback mechanisms, naturally forced by both peak and accumulated boreal summer insolation as well as atmospheric carbon dioxide concentration, have moderated non-linear ice sheet responses to interglacial conditions in the past (Hatfield et al., 2016).

Radiogenic isotope records in minerals isolated from marine sediment from the Eirik Ridge south of Greenland suggest retreat of the southern Greenland Ice Sheet inside the present extent during MIS 5e, MIS 9 and MIS 11, but not MIS 7 (Hatfield et al., 2016). Of these past warm periods, MIS 11 is uniquely suited for comparison with the present interglaciation (MIS 1), with mean atmospheric carbon dioxide concentration similar to pre-industrial Earth (~280 ppm) and comparable insolation parameters to the Holocene (de Vernal & Hillaire-Marcel, 2008; Loutre & Berger, 2003; Raynaud et al., 2005).

The last interglaciation, MIS 5e, is a less powerful analog for future conditions due to greater amplitude of insolation anomalies relative to present natural climate forcing (Robinson et al., 2017). Despite modest natural insolation forcing relative to other Pleistocene interglaciations, marine proxy evidence suggests that the most expansive reduction of the Greenland Ice Sheet during at least the last 600,000 years occurred during MIS 11 (Cluett et al., 2021; de Vernal & Hillaire-Marcel, 2008; Reyes et al., 2014). Spanning ~30,000 years, MIS 11 constitutes an anomalously long interval of interglacial conditions compared to other past warm periods (Tzedakis et al., 2022). Thus, some have hypothesized that the duration of even moderately elevated temperature and atmospheric carbon dioxide concentrations plays an important role in the long-term stability of the Greenland Ice Sheet (Cluett et al., 2021; Tzedakis et al., 2022).

2.2 Terrestrial record of Greenland ecological history

Due to the erosive nature of ice sheets and glaciers, there is a dearth of terrestrial evidence informing Greenland's ecological history beyond the last glaciation. When preserved, organic remains can provide informative constraints for local ecosystem responses to natural climate variability in the past (Figure 1). At present, there are relatively few robust constraints on the depositional timing of known organic remains in Greenland that are older than the limits of radiocarbon dating (~55,000 years) (Hajdas et al., 2021).

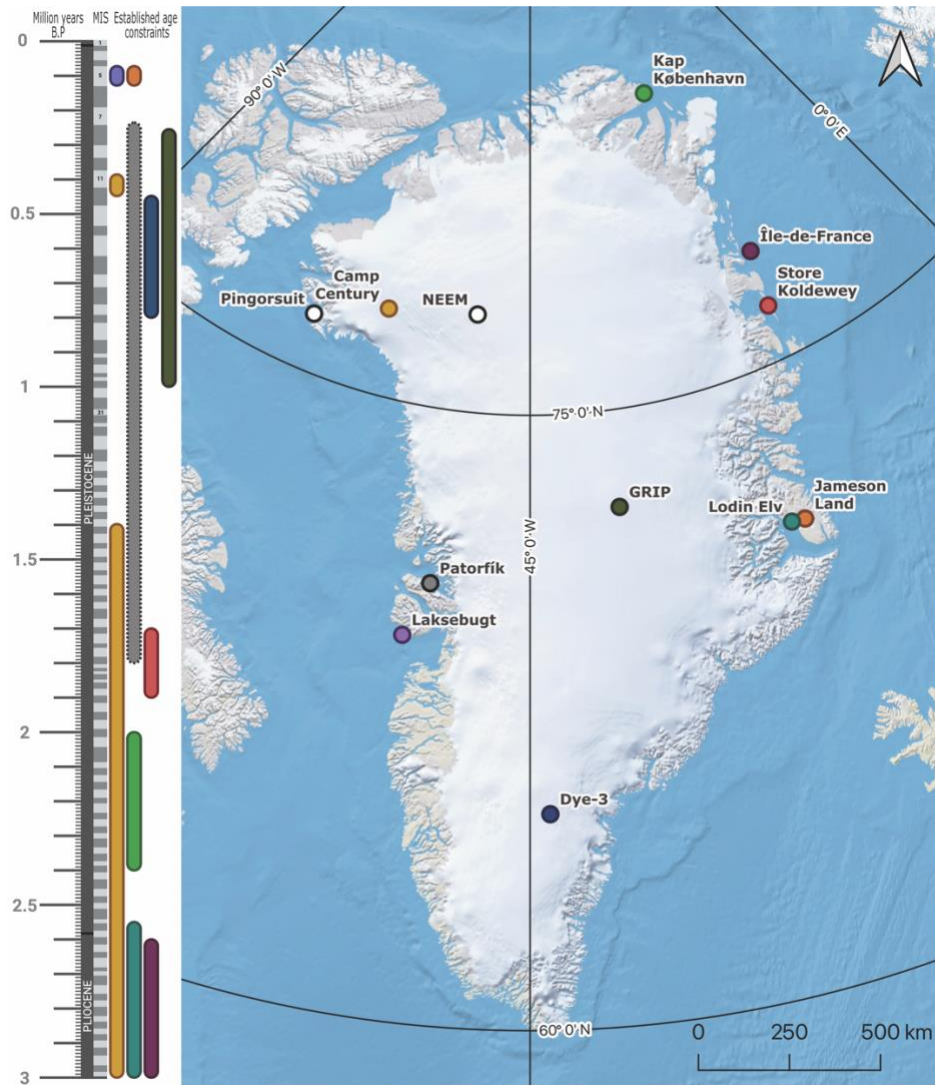


Figure 1. Location of Camp Century and other pre-Holocene organic-bearing deposits in Greenland (right) with established age constraints for each indicated in the corresponding color (left). Marine isotope stage (MIS) boundaries (Lisiecki & Raymo, 2005) are indicated for context (light gray: odd number stage, dark gray: even number stage).

Several rare sediment deposits correlated with Pleistocene and Late Pliocene interglaciations are present in parts of coastal Greenland currently above sea level. The extensively studied Kap København Formation in North Greenland, estimated to be ~2.4 million years old, occupies about 300 km² and is formally classified as two members. The lower member, A, was deposited in a low-energy marine environment with nearby glaciation and contains limited marine fauna consistent with arctic or high arctic conditions (Bennike, 1990; Bennike & Böcher, 1990). The less homogenous upper member B, primarily composed of coastal and nearshore sand, contains terrestrial, marine and limnic macrofossil plant and animal

remains including those with presently sub-arctic distributions (Bennike & Böcher, 1990). These observations, coupled with recent environmental DNA analyses, provide evidence for a warmer climate and distinctly different biotic composition in northern Greenland during the Early Pleistocene (Kjær et al., 2022).

The Store Koldewey, Île-de-France and Lodin-Elv Formations along the East Greenland coast, referred to the Late Pliocene and/or Early Pleistocene, were deposited in shallow ocean environments and contain marine fauna and terrestrial plant remains (Bennike et al., 2001, 2010; Feyling-Hanssen et al., 1983). The Patorfik site in West Greenland, bio- and amino-stratigraphically placed at 235-1800 ka, contains marine fauna characteristic of the subarctic-boreal transition zone (Funder & Simonarson, 1984). A newly exposed sediment deposit near Pingorsuit Glacier in northwestern Greenland, tentatively dated to the Early Pleistocene, contains terrestrial, aquatic and wetland species characteristic of a boreal environment at least 9 °C warmer than present (Bennike et al., 2022). Although these four deposits were likely formed asynchronously based on available age constraints, they offer local insight into periods of warmer temperatures and higher sea levels than present in Greenland beyond the last interglaciation.

Younger deposits found in western, northwestern, and eastern coastal Greenland provide ecological context for the last interglaciation, MIS 5. Animal and herbaceous plant remains from a deposit of shallow marine origin in Narssârssuk, near Thule, indicate summer temperatures ~4°C higher than present (Bennike & Bocher, 1992). Similarly, fossil assemblages from Jameson Land, including a diversity of insects and subarctic terrestrial plant remains, indicate a mean summer temperature ~5°C warmer than present (Bennike & Bocher, 1994).

All organic-bearing deposits discussed thus far are distributed coastally, beyond the present margin of the Greenland Ice Sheet. If organic material is present below the ice sheet, basal sections of deep ice cores can offer more direct insight into local ecological composition when the Greenland Ice Sheet extent was reduced. Biomolecules from basal silty ice of the DYE-3 core suggest the presence of vegetative taxa from the Pinaceae, Taxaceae, Poaceae, Asteraceae and Fabaceae families in southern Greenland at some point between 450-800 ka (Willerslev et al., 2007). Gas isotope fingerprints of methane and oxygen in the basal silty ice of the GRIP core at Summit, central Greenland, are interpreted as vegetation presence and bird activity during formation of the ice sheet (Souchez et al., 2006).

Ratios of organic carbon to total nitrogen (C:N) in sediment extracted from the basal silty ice of the GISP-2 core, also at Summit, central Greenland, indicate the preservation of an ancient tundra soil predating current continent-wide expansion of the ice sheet (Bierman et al., 2014). Recently, stable isotopes of carbon (between -22‰ and -27‰) and C/N ratios (between ~20 and 70) in six sediment samples from the basal ice layer of the NEEM core, reflect presence of an immature tundra or taiga soil during ice-free conditions, though the timing is not well constrained (Blard et al., 2023). Fossil wood is present in one sample from the NEEM basal ice layer (Blard et al., 2023). Notably, every sample in the Camp Century subglacial sediment archive contains intact macrofossils, a robust indicator of former ecosystem presence and species composition.

2.3 Camp Century Subglacial Sediment History

The Camp Century subglacial sediment was recovered ~1,387 meters below the surface of the Greenland Ice Sheet in July 1966 (Hansen & Langway, 1966). Drilling of the third and final borehole at Camp Century, which yielded the first deep ice core to penetrate an entire ice sheet and reach material beneath it, took place from 1963 to 1966 (Hansen & Langway, 1966). The first 535 meters of core were obtained using a thermal drill, replaced by an “Electrodrill” to reach a final depth of 1,391 meters, including ~15.7 meters of debris-laden ice and 3.44 meters of subglacial sediment (Hansen & Langway, 1966; Herron et al., 1979).

At the time, the clean ice section of the Camp Century core was studied extensively. Climatic oscillations spanning the last 100,000-125,000 years are recorded in an oxygen isotope profile measured from ~1600 ice samples throughout the core (Dansgaard et al., 1969). The oxygen isotope variations were compared with a radiocarbon dated pollen study and an oxygen isotope profile from a deep marine sediment core to validate the ice-flow-model-based time-depth assignment (Dansgaard et al., 1969). According to the estimations, prior interglacial ice is preserved in the clean ice of the Camp Century core, implying ice sheet persistence in northwest Greenland during MIS 5 (Weidick, 1975).

The debris-laden basal ice and subglacial sediment were not thoroughly analyzed after collection. Herron and Langway (1979) investigated the composition and physical properties of 16 samples of basal ice, concluding a sub-ice origin of the entrained debris and high levels of deformation down-core. Whalley and Langway (1980) examined surface properties of subglacial

quartz grains, finding both aeolian and subglacial characteristics. Fountain et al. (1981) performed petrographic and isotopic analyses of several cobbles extracted from the subglacial sediment, tentatively concluding a western Greenland origin and 1.1 My age of the sub-ice material. Harwood (1986) analyzed four samples of silty ice and two samples of subglacial sediment, identifying several freshwater diatom species, and providing support for an ice-free northwest Greenland during a previous interglaciation.

The subglacial portion of the frozen archive was removed from the United States in 1994 and stored in a Copenhagen freezer where it was “lost” until resurfacing in 2018, reinvigorating scientific interest in the material. Christ et al. (2021) conducted a multi-proxy pilot study of two subglacial sediment samples, one just below the ice-sediment interface and one at the bottom of the core, using cosmogenic nuclides, infrared-stimulated luminescence (IRSL), geochemistry, scanning electron microscopy, macrofossil characterization, and biomarkers. The two samples suggest at least two periods of ice absence and an older glaciation at Camp Century over the past 3.2 million years (Christ et al., 2021). Further cosmogenic nuclide and IRSL analysis constrained the deposition of the material closest to the ice-sediment interface to 416 ± 38 ka, during MIS 11 (Christ et al., 2023). These initial findings warrant further study of the entire subglacial sediment archive in detail.

3. Objectives

Given the unique opportunity presented by the preservation of organic material within the Camp Century subglacial sediment core, the goal of my thesis work is to address the following questions:

1. What was the composition of emergent ecosystems near Camp Century during the two ice-free periods preserved in the core and are there any systematic differences between them?
2. What environmental and climatic conditions would be necessary to support the development of such ecosystems, e.g., what are the modern distributions of the represented taxa? What temperature and precipitation regimes allow their survival?

4. Methods

My work will address the questions above using multiple proxies for past environmental conditions, including macrofossil characterization, comparative wood anatomical analysis, and organic geochemistry to provide a comprehensive picture of ecosystem development at Camp Century.

4.1 Initial Processing

We isolated organic material and pore ice meltwater from thawed sub-samples (a) and (b) of each core sample (Figure 2). A glass container was used for thawing of sub-sample (b) because I will analyze the pore ice meltwater in this sub-sample for dissolved organic geochemistry. We measured the frozen mass of each sub-sample, thawed the sub-samples overnight in a 4°C refrigerator, and then re-measured the thawed mass to ensure that no water was lost due to evaporation. After thawing, we transferred the sediment into two 250 mL Nalgene bottles that were centrifuged for 20 minutes. The liquid supernatant from sub-sample (b) was transferred into a glass test tube. We recorded the mass of the melted pore ice for both sub-samples. Melted pore ice from sub-sample (b) was transferred to a glass jar and stored frozen at -15 °C.

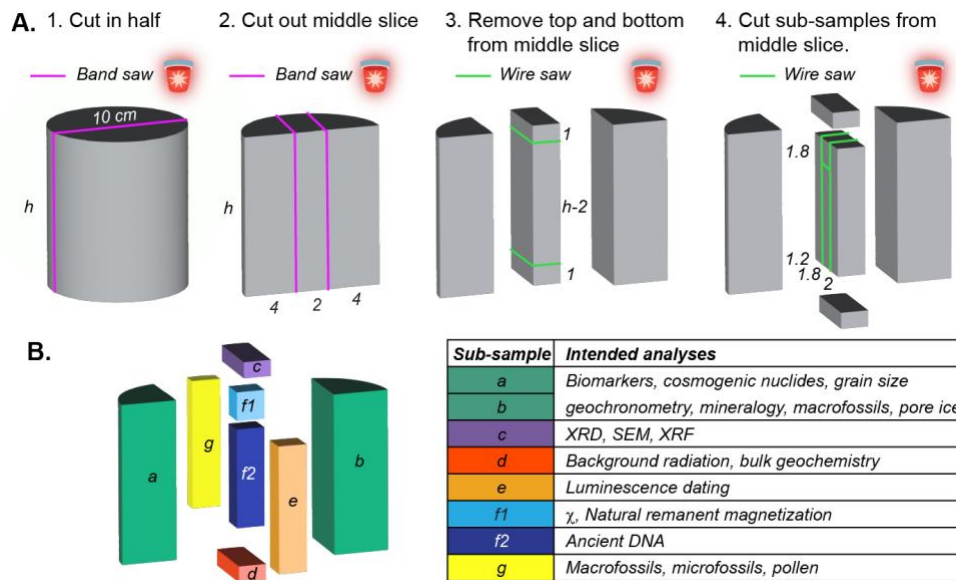


Figure 2. Camp Century subglacial sediment core sub-sampling schematic with typical cutting workflow and intended analyses for respective sub-samples. Source: Bierman et al. (in prep).

We recombined, and gently homogenized the wet, thawed sediment from sub-samples (a) and (b) and recorded the recombined mass. We saved ~10% by mass of the recombined wet sediment, stored at 4°C as wet bulk archive for future biological analyses. Then we wet sieved

the remaining thawed sediment and stored the >2000, 850-2000, 500-850, 250-500, 125-250, and 63-125 μm grain size fractions in plastic bins. For all grain sizes >63 μm , we visually inspected each grain-size fraction and transferred organic material using disposable plastic pipettes into petri dishes for observation and photographic documentation under a dissecting microscope at up to 40x magnification. We transferred organic material from each grain size fraction to glass vials filled with distilled (DI) water for storage at 4°C.

4.2 Macrofossil Characterization

I will identify sufficiently preserved macrofossil specimens from each isolated grain size fraction for each sample to the most specific taxonomic level possible using a combination of reference texts and reference materials. For herbaceous and invertebrate material, I will observe diagnostic features using a dissecting microscope at up to 40x. For bryophytic material, I will mount leaves and if necessary, cross-sections of stem and leaf tissue on microscope slides for examination of cellular features under a light microscope at up to 400x. Following the accepted methods for macrofossil analysis, I will develop a working list of the present taxa and count the number of each taxon in each sample (Figure 3). These counts will ultimately provide a stratigraphic reconstruction of species representation with depth in the sediment core, using the number of individuals counted relative to the known amount of initial sediment for each sample.

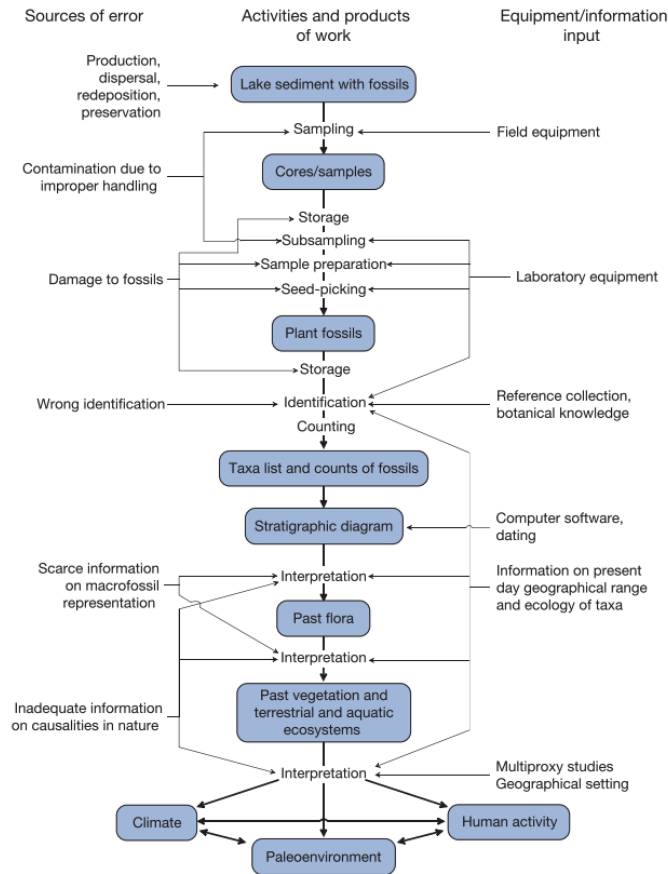


Figure 3. Flowchart showing the typical process of macrofossil analysis in a sediment core. Possible sources of error at each stage (left), successive phases of work (center), and required input (right). Source: Birks (2013)

4.3 Comparative wood anatomical analysis

Presence of woody tissue in macrofossil assemblages can sometimes serve as an indicator of past changes in the latitude or elevation of the northern tree line. The woody tissue present in this core is not identifiable using surface features alone. To address this, I selected 12 specimens of sufficient size (≥ 0.5 mm length) and preservation quality for identification via scanning electron microscopy (SEM) and anatomical analysis from the largest size fractions of isolated macrofossils after wet sieving. I then submerged any non-rigid specimens in liquid nitrogen for 30 seconds to avoid damage during preparation and sectioned all specimens using a new razor blade to expose tangential, longitudinal (radial), and transverse (cross-section) planes of view. Next, I mounted the specimens on SEM stubs lined with adhesive carbon tabs, and sputter coated all stubs with gold-palladium. Using a Tescan Lyra3 GMU FIB SEM, I imaged each plane of view for every specimen at a variety of magnifications. These images provide a view of

diagnostic cellular structures that make it possible to identify each specimen to the genus level, with mentoring from Dr. Barry Rock, a collaborator at the University of New Hampshire.

4.4 Organic geochemistry of bulk organic material

I analyzed bulk organic material (63-250 μm) for $\delta^{15}\text{N}$, $\delta^{13}\text{C}$, total nitrogen content and total carbon content at the University of Washington Isolab using coupled elemental analysis and continuous-flow mass spectrometry. Inclusion in this analysis and the number of replicates possible was limited by the available amount of isolated organic material from each sample. Samples with insufficient organic material for analysis (CC1060-C5, CC1061-A, CC1061-A, CC1061-B, CC1061-C, CC1061-D1, CC1061-D2, CC1061-D3) are all from an ice-rich portion of the core or were missing from the original archive (CC1061-D4, CC1063-3). Samples with sufficient material (n=22) were flash combusted at 1,000 $^{\circ}\text{C}$ with excess oxygen in a Costech ECS 4010 Elemental Analyzer following established methods (Barrie et al., 1989; Verardo et al., 1990). Total nitrogen and carbon are calibrated with a glutamic acid standard with known nitrogen and carbon concentrations. Internal laboratory reference materials (glutamic acid GA1 [$\delta^{13}\text{C}=-28.3\text{‰}$, $\delta^{15}\text{N}=-4.6\text{‰}$], GA2 [$\delta^{13}\text{C}=-13.7\text{‰}$, $\delta^{15}\text{N}=-5.7\text{‰}$], and Salmon [$\delta^{13}\text{C}=-21.33\text{‰}$, $\delta^{15}\text{N}=+11.3\text{‰}$]) were interspersed with samples for calibration. Abundances of carbon and nitrogen stable isotopes are reported using the δ -scale in parts per thousand using the equation,

$$\delta_{\text{sample}}(\text{‰}) = \left(\frac{R_{\text{sample}} - R_{\text{standard}}}{R_{\text{standard}}} \right) * 1000$$

where R_{sample} and R_{standard} are the $^{13}\text{C}/^{12}\text{C}$ or $^{15}\text{N}/^{14}\text{N}$ ratios measured in a sample or standard, respectively. All data are on the Air-N₂ scale, for $\delta^{15}\text{N}$, and the Vienna Pee Dee Belemnite (VPDB) scale, for $\delta^{13}\text{C}$. Precision and accuracy were determined for each run using one of the three references as an unknown (Appendix 2).

The first run included measurement of $\delta^{13}\text{C}$, $\delta^{15}\text{N}$, carbon content and nitrogen content in all 22 samples and duplicates of 13 samples with sufficient material (CC1059-4, CC1059-5b, CC1059-7, CC1060-B, CC1060-C4, CC1062-1, CC1062-2, CC1062-3, CC1062-4, CC1063-4, CC1063-5, CC1063-6, CC1063-8). The second and final run measured $\delta^{13}\text{C}$, carbon content and nitrogen content in 6 samples that either saturated the carbon detector during the first run or had

enough remaining material for another measurement (CC1059-4, CC1060-A1, CC1060-C2, CC1060-C3, CC1059-7, CC1060-D5). Due to limited sample quantities and the low likelihood of carbonate, samples were not acid-washed prior to measurement to avoid loss of material.

4.5 Organic geochemistry of pore water

I will simultaneously measure dissolved organic carbon and total nitrogen concentrations in the pore ice meltwater isolated from sub-sample (b) during initial processing using a Shimadzu TOC-L Total Organic Carbon Analyzer. I will calibrate these measurements using a set of standards with known carbon and nitrogen concentrations. Although the instrument is equipped with an auto-sampling mechanism, I will use a manual injection procedure due to the limited volume of pore ice meltwater available in some samples.

5. Initial Findings

5.1 Organic geochemistry of bulk organic material

I measured $\delta^{13}\text{C}$ vs VPDB (‰), $\delta^{15}\text{N}$ vs Air N_2 (‰), total carbon content (%) and total nitrogen content (%) in December 2022 (Figure 4; Appendix 1,2). Collaborators on the Camp Century subglacial sediment project have identified five distinct stratigraphic units within the core that I use here to report changes in geochemical values with core depth. Unit 1 (n = 12) is the deepest portion of the core characterized as a poorly sorted diamicton containing organic material. Adjacent unit 2 (n=1) is primarily ice with limited sediment and organic material; thus, most samples from this unit were not included in this analysis. Units 3, 4, and 5 (n= 2, 1, and 6, respectively) sequentially decrease in core depth up to the ice-sediment interface, each containing sediments and well-preserved organic material most likely deposited in a fluvial environment. To provide the most complete record possible, I include values for two samples (CC1059-4, CC1063-7) that were measured using the same procedure as part of an earlier pilot study of the Camp Century subglacial sediment core (Christ et al., 2021).

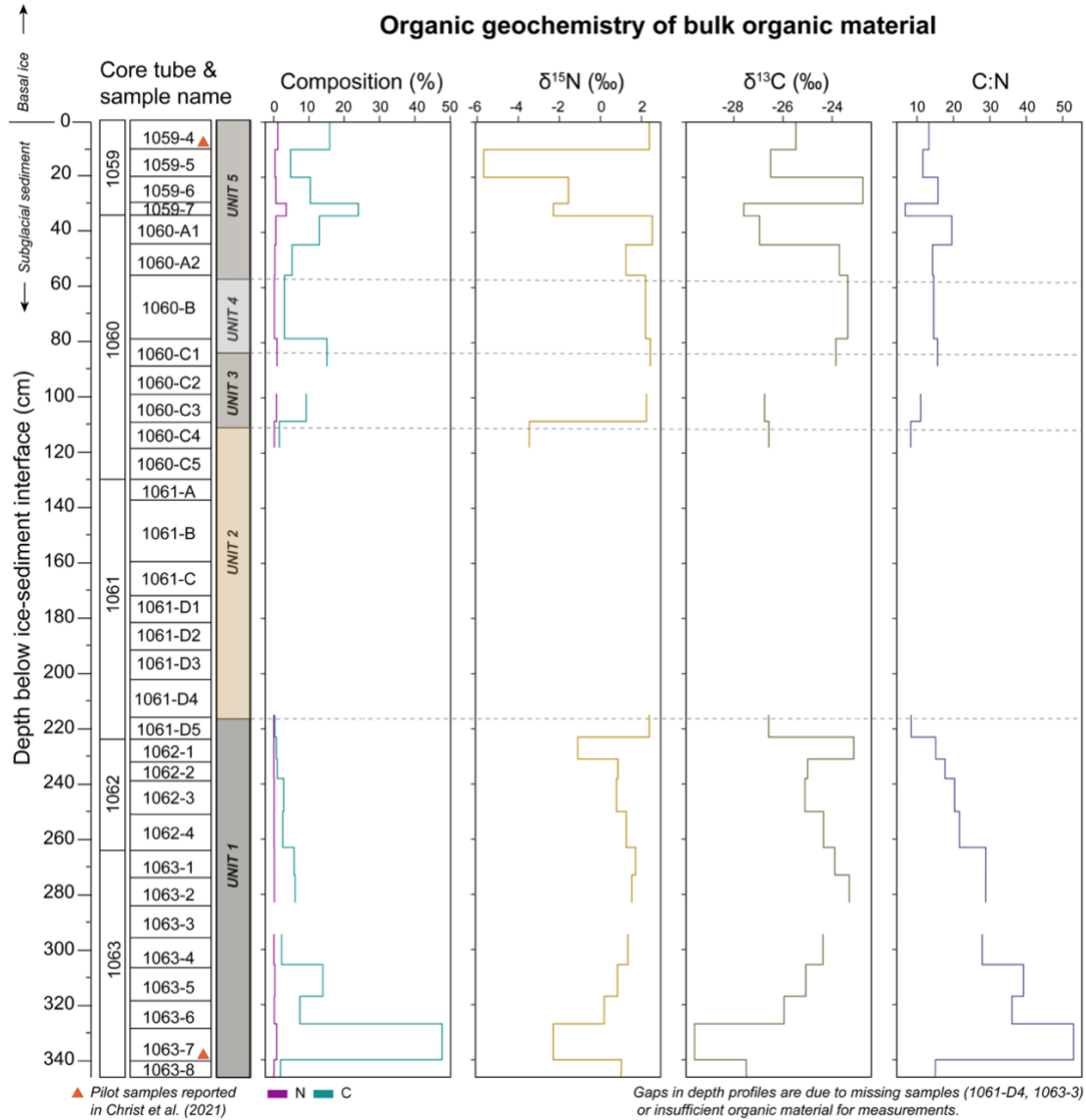


Figure 4. Stable isotope ratios and content of carbon and nitrogen in bulk organic material from the Camp Century subglacial sediment core as related to core depth. Core tube, sample name, and depositional unit classification designated relative to depth.

Carbon/nitrogen ratios (C:N), $\delta^{13}\text{C}$, and $\delta^{15}\text{N}$ can be used to identify the origin and degree of degradation of organic material incorporated in sediments and are often applied in lacustrine and terrestrial environments (Janbu et al., 2011). The context provided by these values is useful in conjunction with characterization of well-preserved microfossil assemblages in case of overrepresentation of species with harder structures relative to less robust organisms that may be more degraded. In the Camp Century subglacial sediments, C:N ratios range from 6 to 53 (Figure 4). In Unit 1, the average C:N ratio is ~25, decreasing up-core in units 3-5 with average C:N

ratios between 13 and 15. Measured $\delta^{13}\text{C}$ values range from -22‰ to -29‰ across the core with average values between -23.4‰ and -25.5‰ for all units and no evident relationship with core depth (Figure 4).

Meyers (1994) identified distinct source combinations of C:N ratios and $\delta^{13}\text{C}$ values for broad classes of organic inputs and found that minor diagenesis did not appreciably impact the two signals in lake or ocean sediments. Applying this comparison, six samples from unit 1 of the Camp Century core fall within the range of C3 land plants as the dominant source of biogenic material to the sediments (Figure 5). One sample each from units 1, 2, and 5 fall within the range of lacustrine algae (Figure 5). Most of the samples lie between the designated ranges of C3 land plants and lacustrine algae, which in the fluviually deposited upper units (3,4,5) could indicate an aquatic environment with both primary production and allochthonous input of terrestrial organic material (Figure 5). The C:N ratios measured in the Camp Century samples are within the ranges of values observed in natural systems, and some of the variability within unit 1 could be due to differences in the maturity or degree of degradation of the organic material (Blard et al., 2023). I plan to measure the same organic geochemical values using bulk sediment, as opposed to isolated organic material, to juxtapose with these measurements and provide a more apt comparison with values measured in arctic soils and other ice core basal materials.

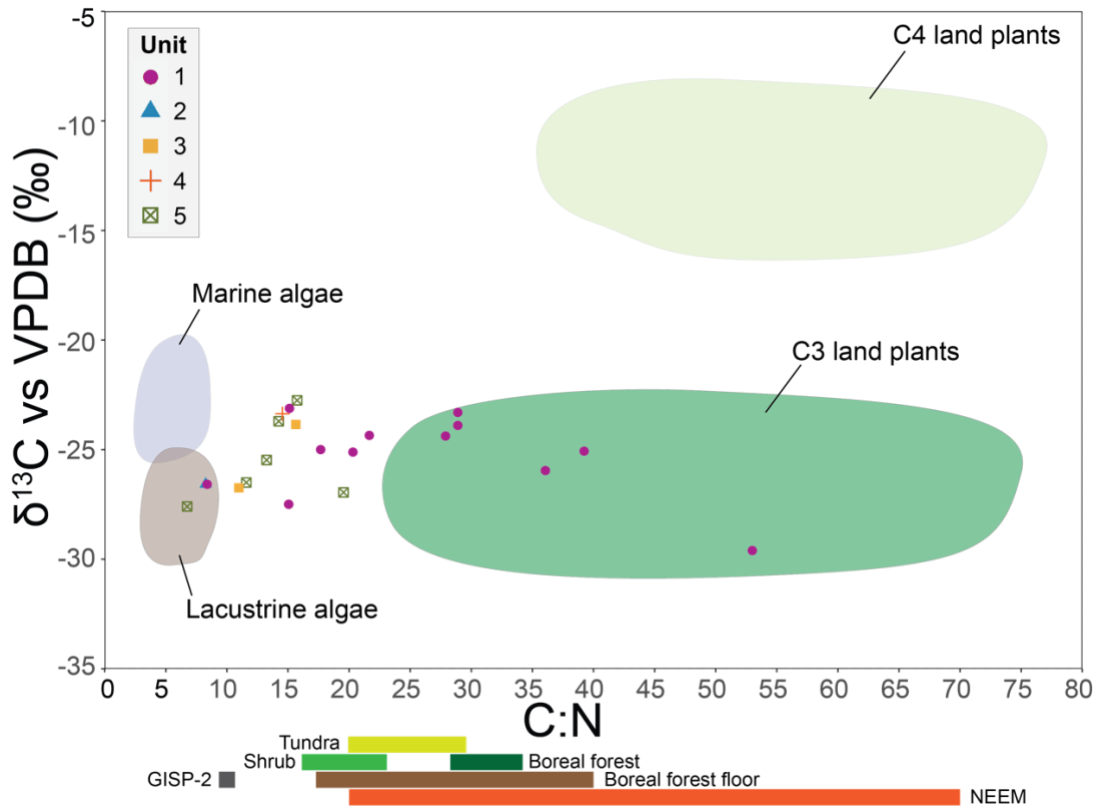


Figure 5. Shaded ranges of source combinations of C:N ratios and $\delta^{13}\text{C}$ values in classes of organic matter. Colored boxes for reference represent measured C:N ratios in soils from tundra, shrub, and boreal forest (Xu et al., 2013), boreal forest floor (Marty et al., 2017), GISP-2 basal material (Bierman, 2014), and NEEM basal material (Blard et al., 2023). Data points are Camp Century subglacial sediment core samples with symbology representing the depositional unit. Modified from: (Meyers, 1994).

The $\delta^{15}\text{N}$ values in Camp Century samples exhibit a wide range from approximately -6‰ to +2‰, with an average value of 0.73 in unit 1 and increased variability up-core. A study of nitrogen dynamics in tundra ecosystems in northern Alaska found that $\delta^{15}\text{N}$ values of the plant species present ranged from -8‰ to +4‰ (Nadelhoffer et al., 1996). The authors attributed this variability in $\delta^{15}\text{N}$ among plant species to partitioning of the available nitrogen pool in response to nutrient limitation, mycorrhizal associations, rooting depth, or differences in plant nitrogen sources (e.g., ammonium, nitrate). In the future, investigating possible covariance among the rest of the measured organic geochemical values could help illuminate primary controls of isotopic variation throughout the core (Janbu et al., 2011).

5.2 Preliminary macrofossil identifications

Organic remains were present in every sample, in varied abundances and levels of preservation. Macrofossils were most limited in unit 2, the ice-rich portion of the core. Upon initial observation, the organic material in unit 1 appears most poorly preserved. The remains include intact ligneous, herbaceous, bryophytic, algal, and invertebrate material. Because quantitative evaluation of the macrofossil record is still in progress, I cannot make any statements about changes in the relative representation of different taxa with core depth. However, preliminary identifications provide a broad view of the material present in the core. Nomenclatural authorities for taxa discussed here are provided in Appendix 3.

The present-day arctic tundra biome is divided into five different bioclimatic sub-zones based on climate and vegetation structure, ranging from 0-3 °C to 9-12 °C mean July temperature from the northernmost point to the boreal tree line (Daniëls, 2015). All five sub-zones are present in modern Greenland, with increased species richness and vascular plant cover along a North-South latitudinal gradient (CAVM Team, 2023). Notable species rich genera in the present-day arctic include *Carex*, *Salix*, *Oxytropis*, *Potentilla*, *Draba*, *Ranunculus*, *Papaver*, *Poa* and *Saxifraga* (Daniëls, 2015).

5.2.1 Notes on select taxa

Observationally, bryophytic remains are dominant relative to other classes of organic material within the core. Remains of *Sphagnum* spp. are represented as leaves in multiple samples in units 1 and 3 (Figure 7A). Stems and leaves of *Scorpidium scorpioides* (hooked scorpion moss) have also been identified in more than one sample in unit 1 (Figure 7B). *S. scorpioides* is a wetland species often found in rich fen environments (Kooijman & Westhoff, 1995). The modern distributions of both *Sphagnum* and *S. scorpioides* in Greenland include widespread coastal areas, although some species in the genus *Sphagnum* are currently restricted to the southern half of Greenland (e.g., *Sphagnum teres*) (Hedenäs & Bennike, 2008).

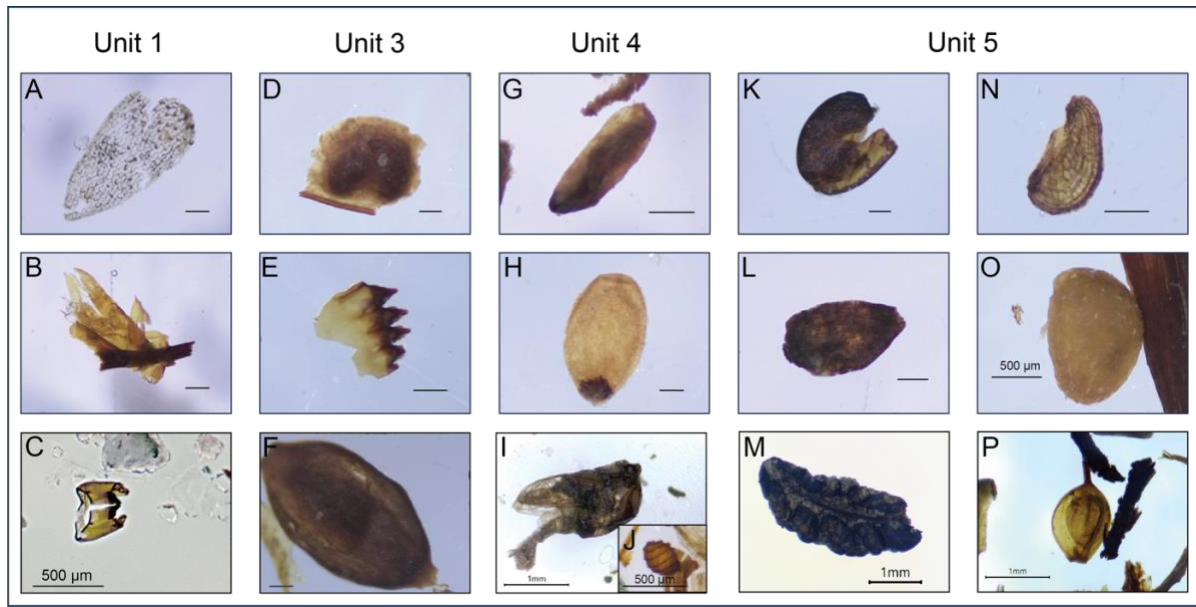


Figure 7. Selection of macrofossil specimens identified in each depositional unit. Scale bars are 200 µm unless otherwise indicated. Occurrence in one depositional unit does not imply absence in the others, as these are preliminary identifications. (A) *Sphagnum* sp. [leaf], (B) *Scorpidium scorpioides* [stem and leaves] (C) Chironomidae [larval head capsule], (D) *Daphnia pulex* [ephippia], (E) *Lepidurus arcticus* [mandible fragment], (F) *Carex* sp. [seed], (G) Poaceae [caryopsis], (H) Juncaceae [seed], (I) Chironomidae [pupa fragment], (J) *Tolypella* sp. [oospore], (K) *Draba* sp. [seed], (L) *Saxifraga* cf. *paniculata* [seed], (M) *Dryas octopetala* [leaf], (N) *Papaver radicans* [seed], (O) *Ranunculus* cf. *hyperboreus* [seed], (P) *Carex* sp. [seed].

Herbaceous and shrub taxa are primarily represented as seeds. At least four seeds of *Papaver radicans* (arctic poppy) are present in the upper core material (Figure 7N). The modern distribution of *P. radicans* is circumpolar with widespread arctic presence (Bay, 1992). A seed and caryopsis of the globally distributed Juncaceae (rush) and Poaceae (grass) families, respectively, are present in unit 4 (Figure 7H, 7G). Seeds of *Carex* spp. (sedge) are present in units 3 and 5 (Figure 7F, 7P). *Carex* is, at present, the most species rich and widespread genus in the Arctic, with species occupying a range of high to low arctic distributions (Bocher, 1951; Hoffmann et al., 2017).

Individual *Draba* sp. (whitlowgrass), *Saxifraga* cf. *paniculata* (alpine saxifrage) and *Ranunculus* cf. *hyperboreus* (arctic buttercup) seeds are present in unit 5 (Figure 7K, 7L, 7O). The genus *Draba* contains ca. 399 extant species, including high-alpine, arctic, and sub-arctic perennials with preferred habitats including coastal shores, rocky outcrops, glacier edges and ice fields (Jordon-Thaden et al., 2013). *S. paniculata* is a perennial, cushion forming arctic-alpine species known to colonize rocky environments, with a modern distribution including Norway,

Iceland, Greenland, and parts of North America and Europe (Reisch, 2008). Remains of *R. hyperboreus* have been reported in other terrestrial deposits in Greenland, and the modern distribution of the species is almost entirely confined to the arctic (Hoffmann et al., 2010).

One leaf of the dwarf shrub, *Dryas octopetala* (eight-petal mountain avens) is present in unit 5 (Figure 7M). *D. octopetala* has a true circumpolar modern distribution including arctic, sub-arctic and alpine areas (Welker et al., 1997). The species is often dominant in vegetative communities in harsh environments, occupying habitats with thin winter snow cover and well-drained summer soils (Welker et al., 1997).

Fragments of freshwater organisms are present in several samples of the core. The non-biting midge (Chironomidae) family is represented as chitinous exoskeletons in both larval and pupal life stages (Figure 7C, 7I). Chironomids are nearly ubiquitous, with species distribution often driven by environmental constraints (Axford et al., 2011). Chironomid assemblages in arctic lake sediments have been compared with modern species distributions to reconstruct paleoclimatic variables including temperature and nutrient status (Axford et al., 2011). Other freshwater invertebrates are represented as a mandible fragment of *Lepidurus arcticus* (tadpole shrimp), and a resting egg pouch of *Daphnia pulex* (water flea) in unit 3 (Figure 7D, 7E). Both species are present in modern ephemeral pools, ponds and shallow lakes in Greenland, and *L. arcticus* has been observed as a predator of *D. pulex* (Christoffersen, 2001). One oospore from the aquatic macroalgae genus *Tolypella* is present in unit 4 (Figure 7J). Only two *Tolypella* species have been observed in water bodies in Greenland (*T. canadensis*, *T. nidifica*), with all documented sightings at or below 70°N (Langangen et al., 1996).

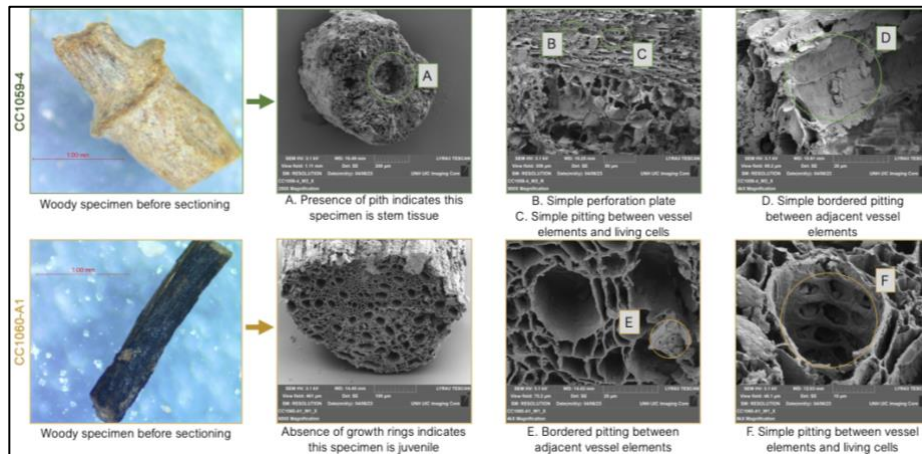


Figure 8. Representative woody tissue specimens and corresponding SEM images with highlighted diagnostic cellular structures.

All sectioned and imaged woody tissue specimens are angiosperms, evidenced by the presence of vessel elements (Figure 8). Absence of growth rings in all specimens could indicate a relatively young age. The presence of a pith in some specimens allowed distinction between root and stem tissue, and there was no clear relationship between the root or stem tissue with core depth. Observations of diagnostic cellular structures including simple perforation plates between vessel elements, simple intervascular pitting between vessel elements and vertical parenchyma cells, and bordered intervascular pitting between adjacent vessel elements support the classification of all specimens as belonging to the genus *Salix* (willow) (Hoadley, 1990).

The modern distributions of all taxa identified in the Camp Century core thus far include or are limited to the arctic tundra biome. Future work including continued identification and observation of changes in species with core depth will provide more detailed insight into ecosystem composition and environmental conditions at the time of deposition.

6. Timeline

Winter 2022 and Spring 2023	<ul style="list-style-type: none"> - Carbon and nitrogen content and stable isotope measurements at UW Isolab (<i>completed</i>) - SEM imaging and identification of viable wood specimens at UNH (<i>completed</i>)
Summer 2023	<ul style="list-style-type: none"> - Seed and invertebrate macrofossil preliminary identifications, advised by Ole Bennike at GEUS (<i>completed</i>) - PaleoCAMP Graduate summer school paleoclimate training (<i>completed</i>)
Fall 2023	<ul style="list-style-type: none"> - Ice Core Analysis Techniques PhD School (<i>completed</i>) - Presentation at RSENR Graduate Research Symposium (<i>completed</i>) - Presentation at Graduate Climate Conference (<i>completed</i>) - Proposal writing and defense (<i>December 2023</i>) - Dissolved organic carbon, total nitrogen measurements in pore ice meltwater at UVM Environmental Geochemistry Lab (<i>in progress</i>) - Presentation at American Geophysical Union Fall Meeting (<i>December 2023</i>)

	- Bulk material stable isotope and C:N measurements (<i>December 2023</i>)
Spring 2024	- Presentation at European Geophysical Union Spring Meeting - Macrofossil counting for quantitative taxa reconstructions (Using reference specimen collection @ Lamont Doherty Earth Observatory, Palisades NY with mentorship from D. Peteet) - Begin writing thesis
Summer 2024	- Continue writing and defend thesis

8. References

- Axford, Y., Briner, J. P., Francis, D. R., Miller, G. H., Walker, I. R., & Wolfe, A. P. (2011). Chironomids record terrestrial temperature changes throughout Arctic interglacials of the past 200,000 yr. *Bulletin of the Geological Society of America*, *123*(7–8), 1275–1287. <https://doi.org/10.1130/B30329.1>
- Barrie, A., Davies, J. E., Park, A. J., & Workman, C. T. (1989). Continuous-flow stable isotope analysis for biologists. *Spectroscopy*, *4*(7), 42–52.
- Bay, C. (1992). A phytogeographical study of the vascular plants of northern Greenland- north of 74 degrees northern latitude. In *Meddelelser om Grønland* (Vol. 36).
- Bennike, O. (1990). The Kap København Formation : stratigraphy and palaeobotany of a Plio-Pleistocene sequence in Peary Land, North Greenland. *Kommissionen for Videnskabelige Undersøgelser i Grønland*, 85.
- Bennike, O., Abrahamsen, N., Bak, M., Israelson, C., Konradi, P., Matthiessen, J., & Witkowski, A. (2001). A multi-proxy study of Pliocene sediments from Ile de France, North-East Greenland. *Palaeogeography, Palaeoclimatology, Palaeoecology*, *186*, 1–23. www.elsevier.com/locate/palaeo
- Bennike, O., & Böcher, J. (1990). Forest-Tundra Neighbouring the North Pole: Plant and Insect Remains from the Plio-Pleistocene Kap København Formation, North Greenland. *Arctic*, *43*(4), 331–338.
- Bennike, O., & Bocher, J. (1992). Early Weichselian interstadial land biotas at Thule, Northwest Greenland. *Boreas*, *21*, 111–117.
- Bennike, O., & Bocher, J. (1994). Land biotas of the last interglacial/glacial cycle on Jameson Land, East Greenland. *Boreas*, *23*, 479–487.
- Bennike, O., Colgan, W., Hedenäs, L., Heiri, O., Lemdahl, G., Wiberg-Larsen, P., Ribeiro, S., Pronzato, R., Manconi, R., & Bjørk, A. A. (2022). An Early Pleistocene interglacial deposit at Pingorsuit, North-West Greenland. *Boreas*. <https://doi.org/10.1111/bor.12596>
- Bennike, O., Knudsen, K. L., Abrahamsen, N., Bocher, J., Cremer, H., & Wagner, B. (2010). Early Pleistocene sediments on Store Koldewey, northeast Greenland. *Boreas*, *39*. <https://doi.org/10.1111/j.1502-3885.2010>
- Berger, B., Crucifix, M., Hodell, D. A., Mangili, C., McManus, J. F., Otto-Bliesner, B., Pol, K., Raynaud, D., Skinner, L. C., Tzedakis, P. C., Wolff, E. W., Yin, Q. Z., Abe-Ouchi, A.,

- Barbante, C., Brovkin, V., Cacho, I., Capron, E., Ferretti, P., Ganopolski, A., ... Vazquez Riveiros, N. (2016). Interglacials of the last 800,000 years. *Reviews of Geophysics*, *54*(1), 162–219. <https://doi.org/10.1002/2015RG000482>
- Bierman, P. R., Corbett, L. B., Graly, J. A., Neumann, T. A., Lini, A., Crosby, B., & Rood, D. H. (2014). Preservation of a preglacial landscape under the center of the Greenland Ice Sheet. *Science*, *344*(6182), 400–402. <https://doi.org/10.1126/science.1250398>
- Birks, H. H. (1993). The importance of plant macrofossils in late-glacial climatic reconstructions: An example from Western Norway. *Quaternary Science Reviews*, *12*, 719–726.
- Birks, H. H. (2013). Plant Macrofossil Introduction. In *Encyclopedia of Quaternary Science: Second Edition* (pp. 593–612). Elsevier Inc. <https://doi.org/10.1016/B978-0-444-53643-3.00203-X>
- Blard, P.-H., Protin, M., Tison, J.-L., Fripiat, F., Dahl-Jensen, D., Steffensen, J. P., Mahaney, W. C., Bierman, P. R., Christ, A. J., Corbett, L. B., Debaille, V., Rigaudier, T., & Claeys, P. (2023). Basal debris of the NEEM ice core, Greenland: a window into sub-ice-sheet geology, basal ice processes and ice-sheet oscillations. *Journal of Glaciology*, 1–19. <https://doi.org/10.1017/jog.2022.122>
- Bocher, T. W. (1951). Distributions of Plants in the Circumpolar Area in Relation to Ecological and Historical Factors. *Journal of Ecology*, *39*(2), 376–395. <https://about.jstor.org/terms>
- Box, J. E., Hubbard, A., Bahr, D. B., Colgan, W. T., Fettweis, X., Mankoff, K. D., Wehrlé, A., Noël, B., van den Broeke, M. R., Wouters, B., Björk, A. A., & Fausto, R. S. (2022). Greenland ice sheet climate disequilibrium and committed sea-level rise. *Nature Climate Change*. <https://doi.org/10.1038/s41558-022-01441-2>
- Briner, J. P., Cuzzone, J. K., Badgeley, J. A., Young, N. E., Steig, E. J., Morlighem, M., Schlegel, N. J., Hakim, G. J., Schaefer, J. M., Johnson, J. V., Lesnek, A. J., Thomas, E. K., Allan, E., Bennike, O., Cluett, A. A., Csatho, B., de Vernal, A., Downs, J., Larour, E., & Nowicki, S. (2020). Rate of mass loss from the Greenland Ice Sheet will exceed Holocene values this century. *Nature*, *586*(7827), 70–74. <https://doi.org/10.1038/s41586-020-2742-6>
- CAVM Team. (2023). Raster Circumpolar Arctic Vegetation Map. Scale 1:7,000,000. *Conservation of Arctic Flora and Fauna*. doi:10.18739/A2RX93F75
- Christ, A. J., Bierman, P. R., Schaefer, J. M., Dahl-Jensen, D., Steffensen, J. P., Corbett, L. B., Peteet, D. M., Thomas, E. K., Steig, E. J., Rittenour, T. M., Tison, J.-L., Blard, P.-H., Perdrial, N., Dethier, D. P., Lini, A., Hidy, A. J., Caffee, M. W., & Southon, J. (2021). A multimillion-year-old record of Greenland vegetation and glacial history preserved in sediment beneath 1.4 km of ice at Camp Century. *PNAS*, *118*(13). <https://doi.org/10.1073/pnas.2021442118/-/DCSupplemental>
- Christ, A. J., Rittenour, T. M., Bierman, P. R., Keisling, B. A., Knutz, P. C., Thomsen, T. B., Keulen, N., Fosdick, J. C., Hemming, S. R., Tison, J.-L., Blard, P.-H., Steffensen, J. P., Caffee, M. W., Corbett, L. B., Dahl-Jensen, D., Dethier, D. P., Hidy, A. J., Perdrial, N., Peteet, D. M., ... Thomas, E. K. (2023). Deglaciation of northwestern Greenland during Marine Isotope Stage 11. *Science*, *1063*. <https://www.science.org>
- Christoffersen, K. (2001). Predation on *Daphnia pulex* by *Lepidurus arcticus*. *Hydrobiologia*, *442*, 223–229.
- Cluett, A. A., Thomas, E. K., & Freeman, K. H. (2021). Summer warmth of the past six interglacials on Greenland. *PNAS*, *118*(20), 1–6. <https://doi.org/10.1073/pnas.2022916118/-/DCSupplemental>

- Crump, S. E., Fréchette, B., Power, M., Cutler, S., De Wet, G., Raynolds, M. K., Raberg, J. H., Briner, J. P., Thomas, E. K., Sepúlveda, J., Shapiro, B., Bunce, M., Miller, G. H., Performed, J. S., & Analyzed, J. P. B. (2021). Ancient plant DNA reveals High Arctic greening during the Last Interglacial. *PNAS*, *118*.
<https://doi.org/10.1073/pnas.2019069118/-/DCSupplemental>
- Daniëls, F. J. A. (2015). A review of anthropogenic changes in the vascular plant flora and vegetation of the Arctic with special reference to Greenland. *Braunschweiger Geobotanische Arbeiten*, *11*, 77–98. <https://www.researchgate.net/publication/282443273>
- Dansgaard, W., Johnsen, S. J., Møller, J., & Langway, C. C. (1969). One Thousand Centuries of Climatic Record from Camp Century. *Science*, *166*(3903), 377–380.
- de Vernal, A., & Hillaire-Marcel, C. (2008). Natural Variability of Greenland Climate, Vegetation, and Ice Volume During the Past Million Years. *Science*, *320*(5883), 1622–1625. <https://doi.org/10.1126/science.1157166>
- Dutton, A., Carlson, A. E., Long, A. J., Milne, G. A., Clark, P. U., DeConto, R., Horton, B. P., Rahmstorf, S., & Raymo, M. E. (2015). Sea-level rise due to polar ice-sheet mass loss during past warm periods. *Science*, *349*(6244). <https://doi.org/10.1126/science.aaa4019>
- Elderfield, H., Ferretti, P., Greaves, M., Crowhurst, S., Mccave, I. N., Hodell, D., & Piotrowski, A. M. (2012). Evolution of Ocean Temperature and Ice Volume Through the Mid-Pleistocene Climate Transition. *Science*, *337*. <https://doi.org/10.1594/PANGAEA.786205>
- Elmendorf, S. C., Henry, G. H. R., Hollister, R. D., Björk, R. G., Boulanger-Lapointe, N., Cooper, E. J., Cornelissen, J. H. C., Day, T. A., Dorrepaal, E., Elumeeva, T. G., Gill, M., Gould, W. A., Harte, J., Hik, D. S., Hofgaard, A., Johnson, D. R., Johnstone, J. F., Jónsdóttir, I. S., Jørgenson, J. C., ... Wipf, S. (2012). Plot-scale evidence of tundra vegetation change and links to recent summer warming. *Nature Climate Change*, *2*(6), 453–457. <https://doi.org/10.1038/nclimate1465>
- Feyling-Hanssen, R. W., Funder, S., & Petersen, K. S. (1983). The Lodin Elv Formation; a Pliocene occurrence in Greenland. *Bull. Geol. Soc. Denmark*, *31*, 81–106.
<https://www.researchgate.net/publication/282269942>
- Forkel, M., Carvalhais, N., Rödenbeck, C., Keeling, R., Heimann, M., Thonicke, K., Zaehle, S., & Reichstein, M. (2016). Enhanced seasonal CO₂ exchange caused by amplified plant productivity in northern ecosystems. *Science*, *351*(6247).
<https://doi.org/10.1126/science.aac4971>
- Funder, S., Abrahamsen, N., Bennike, O., & Feyling-Hanssen, R. W. (1985). Forested Arctic: evidence from north Greenland. *Geology*, *13*, 542–546.
- Funder, S., Bennike, O., Böcher, J., Israelson, C., Símonarson, L. A., & Petersen, C. (2001). Late Pliocene Greenland-The Kap København Formation in North Greenland. *Bulletin of the Geological Society of Denmark*, *48*, 117–134.
- Funder, S., & Simonarson, L. R. (1984). Bio- and aminostratigraphy of some Quaternary marine deposits in West Greenland. *Canadian Journal of Earth Sciences*, *21*(7), 843–852.
<https://doi.org/10.1139/e84-090>
- Hajdas, I., Ascough, P., Garnett, M. H., Fallon, S. J., Pearson, C. L., Quarta, G., Spalding, K. L., Yamaguchi, H., & Yoneda, M. (2021). Radiocarbon dating. *Nature Reviews Methods Primers*, *1*(1). <https://doi.org/10.1038/s43586-021-00058-7>
- Hansen, B. L., & Langway, C. C. (1966). Deep Core Drilling in Ice and Core Analysis at Camp Century, Greenland, 1961-1966. *Glaciology*, 207–208.

- Harwood, D. M. (1986). Do Diatoms beneath the Greenland Ice Sheet Indicate Interglacials Warmer than Present? *Arctic*, 39(4), 304–308.
- Hatfield, R. G., Reyes, A. V., Stoner, J. S., Carlson, A. E., Beard, B. L., Winsor, K., & Welke, B. (2016). Interglacial responses of the southern Greenland ice sheet over the last 430,000 years determined using particle-size specific magnetic and isotopic tracers. *Earth and Planetary Science Letters*, 454, 225–236. <https://doi.org/10.1016/j.epsl.2016.09.014>
- Hedenäs, L., & Bennike, O. (2008). A Plio-Pleistocene moss assemblage from Store Koldewey, NE Greenland. *Lindbergia*, 33(1), 23–37. <https://www.jstor.org/stable/27809535>
- Herron, S., Hoar, & Langway, C. C. (1979). The Debris-Laden Ice at the Bottom of the Greenland Ice Sheet. *Journal of Glaciology*, 23(89), 193–207. <https://doi.org/10.3189/s002214300002983x>
- Hoadley, B. (1990). *Identifying Wood*. Taunton Press.
- Hofer, S., Lang, C., Amory, C., Kittel, C., Delhasse, A., Tedstone, A., & Fettweis, X. (2020). Greater Greenland Ice Sheet contribution to global sea level rise in CMIP6. *Nature Communications*, 11(1). <https://doi.org/10.1038/s41467-020-20011-8>
- Hoffmann, M. H., Gebauer, S., & von Rozycki, T. (2017). Assembly of the Arctic flora: Highly parallel and recurrent patterns in sedges (*Carex*). *American Journal of Botany*, 104(9), 1334–1343. <https://doi.org/10.3732/ajb.1700133>
- Hoffmann, M. H., Von Hagen, K. B., Hörandl, E., Röser, M., & Tkach, N. V. (2010). Sources of the arctic flora: Origins of arctic species in ranunculus and related genera. *International Journal of Plant Sciences*, 171(1), 90–106. <https://doi.org/10.1086/647918>
- IPCC. (2022). Summary for Policymakers. In H.-O. Pörtner, D. C. Roberts, M. Tignor, E. S. Poloczanska, K. Mintenbeck, A. Alegría, M. Craig, S. Langsdorf, S. Löschke, V. Möller, A. Okem, & B. Rama (Eds.), *Climate Change 2022: Impacts, Adaptation, and Vulnerability. Contribution of Working Group II to the Sixth Assessment Report of the Intergovernmental Panel on Climate Change* (pp. 3–33). Cambridge University Press. <https://doi.org/10.1017/9781009325844.001>
- Irvali, N., Galaasen, E. V., Ninnemann, U. S., Rosenthal, Y., Born, A., & Kleiven, H. F. (2020). A low climate threshold for south Greenland Ice Sheet demise during the Late Pleistocene. *PNAS*, 117(1), 190–195. <https://doi.org/10.1073/pnas.1911902116/-/DCSupplemental>
- Janbu, A. D., Paasche, Y., & Talbot, M. R. (2011). Paleoclimate changes inferred from stable isotopes and magnetic properties of organic-rich lake sediments in Arctic Norway. *Journal of Paleolimnology*, 46(1), 29–44. <https://doi.org/10.1007/s10933-011-9512-2>
- Fountain, J., Usselman, T. M., Wooden, J., & Langway, C. C. (1981). Evidence of the bedrock beneath the Greenland Ice Sheet near Camp Century, Greenland. *Journal of Glaciology*, 27(95), 193–197.
- Jordon-Thaden, I. E., Al-Shehbaz, I. A., & Koch, M. A. (2013). Species richness of the globally distributed, arctic-alpine genus *Draba* L. (Brassicaceae). *Alpine Botany*, 123(2), 97–106. <https://doi.org/10.1007/s00035-013-0120-9>
- Kjær, K. H., Winther Pedersen, M., De Sanctis, B., De Cahsan, B., Korneliussen, T. S., Michelsen, C. S., Sand, K. K., Jelavić, S., Ruter, A. H., Schmidt, A. M. A., Kjeldsen, K. K., Tesakov, A. S., Snowball, I., Gosse, J. C., Alsos, I. G., Wang, Y., Dockter, C., Rasmussen, M., Jørgensen, M. E., ... Willerslev, E. (2022). A 2-million-year-old ecosystem in Greenland uncovered by environmental DNA. *Nature*, 612(7939), 283–291. <https://doi.org/10.1038/s41586-022-05453-y>

- Kooijman, A. M., & Westhoff, V. (1995). Variation in habitat factors and species composition of *Scorpidium scorpioides* communities in NW-Europe. *Vegetatio*, *117*, 133–150.
- Langangen, A., Hansen, J. B., & Mann, H. (1996). The charophytes of Greenland. *Cryptogamie, Algol.*, *17*(4), 293–257.
- Lawrence, D. M., & Swenson, S. C. (2011). Permafrost response to increasing Arctic shrub abundance depends on the relative influence of shrubs on local soil cooling versus large-scale climate warming. *Environmental Research Letters*, *6*(4). <https://doi.org/10.1088/1748-9326/6/4/045504>
- Lisiecki, L. E., & Raymo, M. E. (2005). A Pliocene-Pleistocene stack of 57 globally distributed benthic δ 18O records. *Paleoceanography*, *20*(1), 1–17. <https://doi.org/10.1029/2004PA001071>
- Loutre, M. F., & Berger, A. (2003). Marine Isotope Stage 11 as an analogue for the present interglacial. *Global and Planetary Change*, *36*(3), 209–217. [https://doi.org/10.1016/S0921-8181\(02\)00186-8](https://doi.org/10.1016/S0921-8181(02)00186-8)
- Marty, C., Houle, D., Gagnon, C., & Courchesne, F. (2017). The relationships of soil total nitrogen concentrations, pools and C:N ratios with climate, vegetation types and nitrate deposition in temperate and boreal forests of eastern Canada. *Catena*, *152*, 163–172. <https://doi.org/10.1016/j.catena.2017.01.014>
- Mekonnen, Z. A., Riley, W. J., & Grant, R. F. (2018). 21st century tundra shrubification could enhance net carbon uptake of North America Arctic tundra under an RCP8.5 climate trajectory. In *Environmental Research Letters* (Vol. 13, Issue 5). Institute of Physics Publishing. <https://doi.org/10.1088/1748-9326/aabf28>
- Meyers, P. A. (1994). Preservation of elemental and isotopic source identification of sedimentary organic matter. *Chemical Geology*, *114*, 289–302.
- Myers-Smith, I. H., Kerby, J. T., Phoenix, G. K., Bjerke, J. W., Epstein, H. E., Assmann, J. J., John, C., Andreu-Hayles, L., Angers-Blondin, S., Beck, P. S. A., Berner, L. T., Bhatt, U. S., Bjorkman, A. D., Blok, D., Bryn, A., Christiansen, C. T., Cornelissen, J. H. C., Cunliffe, A. M., Elmendorf, S. C., ... Wipf, S. (2020). Complexity revealed in the greening of the Arctic. *Nature Climate Change*, *10*(2), 106–117. <https://doi.org/10.1038/s41558-019-0688-1>
- Myneni, R. B., Keeling, C. D., Tucker, C. J., Asrar, G., & Nemani, R. R. (1997). Increased plant growth in the northern high latitudes from 1981 to 1991. *Nature*, *386*, 698–701.
- Nadelhoffer, K., Shaver, G., Fry, B., Giblin, A., Johnson, L., & McKane R. (1996). 15N natural abundances and N use by tundra plants. *Oecologia*, *107*, 386–394.
- Pearson, R. G., Phillips, S. J., Lorant, M. M., Beck, P. S. A., Damoulas, T., Knight, S. J., & Goetz, S. J. (2013). Shifts in Arctic vegetation and associated feedbacks under climate change. *Nature Climate Change*, *3*(7), 673–677. <https://doi.org/10.1038/nclimate1858>
- Post, E., Alley, R. B., Christensen, T. R., Macias-Fauria, M., Forbes, B. C., Gooseff, M. N., Iler, A., Kerby, J. T., Laidre, K. L., Mann, M. E., Olofsson, J., Stroeve, J. C., Ulmer, F., Virginia, R. A., & Wang, M. (2019). The polar regions in a 2°C warmer world. *Sci. Adv.*, *5*. <https://data>.
- Rantanen, M., Karpechko, A. Y., Lipponen, A., Nordling, K., Hyvärinen, O., Ruosteenoja, K., Vihma, T., & Laaksonen, A. (2022). The Arctic has warmed nearly four times faster than the globe since 1979. *Communications Earth and Environment*, *3*(1). <https://doi.org/10.1038/s43247-022-00498-3>

- Raynaud, D., Barnola, J.-M., Souchez, R., Lorrain, R., Petit, J.-R., Duval, P., & Lipenkov, V. Y. (2005). The record for marine isotopic stage 11. *Nature*, *436*.
- Reisch, C. (2008). Glacial history of *Saxifraga paniculata* (Saxifragaceae): molecular biogeography of a disjunct arctic-alpine species from Europe and North America. *Biological Journal of the Linnean Society*, *93*, 385–398. <https://academic.oup.com/biolinnean/article/93/2/385/2701276>
- Reyes, A. V., Carlson, A. E., Beard, B. L., Hatfield, R. G., Stoner, J. S., Winsor, K., Welke, B., & Ullman, D. J. (2014). South Greenland ice-sheet collapse during Marine Isotope Stage 11. *Nature*, *510*(7506), 525–528. <https://doi.org/10.1038/nature13456>
- Robinson, A., Alvarez-Solas, J., Calov, R., Ganopolski, A., & Montoya, M. (2017). MIS-11 duration key to disappearance of the Greenland ice sheet. *Nature Communications*, *8*. <https://doi.org/10.1038/ncomms16008>
- Schaeffer, S. M., Sharp, E., Schimel, J. P., & Welker, J. M. (2013). Soil-plant N processes in a High Arctic ecosystem, NW Greenland are altered by long-term experimental warming and higher rainfall. *Global Change Biology*, *19*(11), 3529–3539. <https://doi.org/10.1111/gcb.12318>
- Souchez, R., Jouzel, J., Landais, A., Chappellaz, J., Lorrain, R., & Tison, J. L. (2006). Gas isotopes in ice reveal a vegetated central Greenland during ice sheet invasion. *Geophysical Research Letters*, *33*(24). <https://doi.org/10.1029/2006GL028424>
- Steig, E. J., & Wolfe, A. P. (2008). Sprucing up Greenland. *Science*, *320*(5883), 1595–1596. <https://doi.org/10.1126/science.1160004>
- Stone, E. J., & Lunt, D. J. (2013). The role of vegetation feedbacks on Greenland glaciation. *Climate Dynamics*, *40*(11–12), 2671–2686. <https://doi.org/10.1007/s00382-012-1390-4>
- Sturm, M., Mcfadden, J. P., Liston, G. E., Stuart Chapin Iii, # F, Racine, C. H., & Holmgren, J. (2001). Snow-Shrub Interactions in Arctic Tundra: A Hypothesis with Climatic Implications. *Journal of Climate*, *14*, 336–344.
- Swann, A. L., Fung, I. Y., Levis, S., Bonan, G. B., & Doney, S. C. (2010). Changes in arctic vegetation amplify high-latitude warming through the greenhouse effect. *Proceedings of the National Academy of Sciences of the United States of America*, *107*(4), 1295–1300. <https://doi.org/10.1073/pnas.0913846107>
- Tzedakis, P. C., Hodell, D. A., Nehrbass-Ahles, C., Mitsui, T., & Wolff, E. W. (2022). Marine Isotope Stage 11c: An unusual interglacial. *Quaternary Science Reviews*, *284*. <https://doi.org/10.1016/j.quascirev.2022.107493>
- Verardo, D. J., Froelich, P. N., & McIntyre, A. (1990). Determination of organic carbon and nitrogen in marine sediments using the Carlo Erba NA-1500 Analyzer. *Deep-Sea Research*, *37*(1), 157–165.
- Wagner, B., & Bennike, O. (2012). Chronology of the last deglaciation and Holocene environmental changes in the Sisimiut area. *Boreas*, *41*(10), 481–493. <https://doi.org/10.1111/j.1502>
- Weidick, A. (1975). *A Review of Quaternary Investigations in Greenland*.
- Welker, J. M., Molau, U., Parsons, A. N., Robinson, C. H., & Wookey, P. A. (1997). Responses of *Dryas octopetala* to ITEX environmental manipulations: A synthesis with circumpolar comparisons. *Global Change Biology*, *3*(SUPPL. 1), 61–73. <https://doi.org/10.1111/j.1365-2486.1997.gcb143.x>

- Whalley, W. B., & Langway, C. C. (1980). A Scanning Electron Microscope Examination of Subglacial Quartz Grains from Camp Century Core, Greenland—A Preliminary Study. *Journal of Glaciology*, 25(91), 125–132. <https://doi.org/10.3189/s0022143000010340>
- Willerslev, E., Capellini, E., Boomsma, W., Nielsen, R., Hebsgaard, M. B., Brand, T. B., Hofreiter, M., Bunce, M., Poinar, H. N., Dahl-Jensen, D., Johnsen, S., Steffensen, J. P., Bennike, O., Schwenninger, J. L., Nathan, R., Armitage, S., de Hoog, C. J., Alfimov, V., Christl, M., ... Collins, M. J. (2007). Ancient Biomolecules from Deep Ice Cores Reveal a Forested Southern Greenland. *Journal of Geophysical Research*, 108(B8), 111–113. <https://doi.org/10.1029/2002jb002233>
- Xu, X., Thornton, P. E., & Post, W. M. (2013). A global analysis of soil microbial biomass carbon, nitrogen and phosphorus in terrestrial ecosystems. *Global Ecology and Biogeography*, 22(6), 737–749. <https://doi.org/10.1111/geb.12029>

Appendix:

Appendix 1. Summary of geochemical measurements in bulk organic material (*: includes pilot data, NA: insufficient material for analysis, bold sample name: includes data from carbon-only run).

Sample	Number of replicates	Depth of sample top (cm)	[N] (%)	$\delta^{15}\text{N}$ vs Air N_2 (‰)	[C] (%)	$\delta^{13}\text{C}$ vs VPDB (‰)	C:N
CC1059-4	3*	0	1.20%	2.38	15.86%	-25.48	13.25
CC1059-5b	2	10	0.41%	-5.68	4.80%	-26.50	11.59
CC1059-6	1	20	0.66%	-1.56	10.42%	-22.75	15.75
CC1059-7	3	29.5	3.56%	-2.29	24.00%	-27.60	6.75
CC1060-A1	1	34	0.66%	2.52	12.96%	-26.95	19.54
CC1060-A2	1	44.5	0.37%	1.24	5.22%	-23.71	14.24
CC1060-B	2	55.5	0.21%	2.19	3.06%	-23.37	14.55
CC1060-C1	1	78.5	0.97%	2.43	15.11%	-23.85	15.64
CC1060-C2	NA	88.5	NA	NA	NA	NA	NA
CC1060-C3	1	98.5	0.84%	2.24	9.26%	-26.75	10.97
CC1060-C4 Sed	2	108.5	0.20%	-3.46	1.61%	-26.58	8.26
CC1060-C5	NA	118	NA	NA	NA	NA	NA
CC1061-A	NA	129	NA	NA	NA	NA	NA
CC1061-B	NA	137	NA	NA	NA	NA	NA
CC1061-C	NA	159	NA	NA	NA	NA	NA
CC1061-D1	NA	171	NA	NA	NA	NA	NA
CC1061-D2	NA	181	NA	NA	NA	NA	NA
CC1061-D3	NA	191	NA	NA	NA	NA	NA
CC1061-D4ice	NA	201	NA	NA	NA	NA	NA

CC1061-D4rock	NA	207	NA	NA	NA	NA	NA
CC1061-D5	2	215	0.041%	2.38	0.34%	-26.58	8.37
CC1062-1	2	223	0.053%	-1.10	0.80%	-23.12	15.12
CC1062-2	2	231	0.060%	0.85	1.06%	-25.00	17.67
CC1062-3	2	238	0.14%	0.78	2.87%	-25.11	20.31
CC1062-4	2	250	0.12%	1.26	2.63%	-24.35	21.66
CC1063-1	1	263	0.20%	1.71	5.81%	-23.90	28.90
CC1063-2	1	273	0.21%	1.53	6.11%	-23.30	28.89
CC1063-3	NA	283	NA	NA	NA	NA	NA
CC1063-4	2	294.5	0.081%	1.34	2.26%	-24.38	27.89
CC1063-5	2	305.5	0.36%	0.83	13.94%	-25.07	39.24
CC1063-6	2	317	0.21%	0.18	7.46%	-25.96	36.07
CC1063-7	1*	327	0.90%	-2.3	47.70%	-29.60	53.00
CC1063-8	2	340	0.13%	1.02	1.95%	-27.50	15.05

Appendix 2. Accuracy and precision for multiple runs included in organic geochemical analysis determined using internal reference materials with known values (GA1, GA2, Salmon) at the University of Washington Isolab.

Run of instrument	[N] (%)		[C] (%)		$\delta^{13}\text{C}$ vs VPDB (‰)		$\delta^{15}\text{N}$ vs Air N_2 (‰)	
	Accuracy	Precision	Accuracy	Precision	Accuracy	Precision	Accuracy	Precision
2021 pilot carbon and nitrogen	-0.058	0.26	-0.18	0.71	0.023	0.074	-0.070	0.16
Carbon and nitrogen	-0.15	0.25	-0.30	1.03	0.11	0.25	-0.019	0.24
Carbon-only	NA	NA	1.59	0.50	0.55	0.73	NA	NA

Appendix 3. Nomenclatural authorities for taxa mentioned in text

<i>Carex</i> L.
<i>Draba</i> L.
<i>Dryas octopetala</i> L.
<i>Papaver radicum</i> auct. coll.
<i>Ranunculus hyperboreus</i> Rottb.
<i>Saxifraga paniculata</i> Mill.
<i>Scorpidium scorpioides</i> (Hedw.) Limpr.
<i>Sphagnum</i> L.
<i>Salix</i> L.

<i>Sphagnum teres</i> Schimp.
<i>Lepidurus arcticus</i> (Pallas, 1793)
<i>Daphnia pulex</i> (Leydig, 1860)
<i>Tolypella canadensis</i> Sawa
<i>Tolypella nidifica</i> (O.F.Müll.) Leonh.